

# Temperature Dependence of Three-Terminal Molecular Junctions with Sulfur End-Functionalized Tercyclohexylidenes

Menno Poot,<sup>†</sup> Edgar Osorio,<sup>†</sup> Kevin O'Neill,<sup>†</sup> Jos M. Thijssen,<sup>†</sup>  
Daniel Vanmaekelbergh,<sup>‡</sup> Cornelis A. van Walree,<sup>§</sup>  
Leonardus W. Jenneskens,<sup>§</sup> and Herre S. J. van der Zant<sup>\*,†</sup>

*Kavli Institute of Nanoscience, Delft University of Technology, P.O. Box 5046, 2600 GA, The Netherlands, Condensed Matter and Interfaces, Utrecht University, Princetonplein 1, 3584 CC Utrecht, The Netherlands, and Organic Chemistry and Catalysis, Utrecht University, Padualaan 8, 3584 CH Utrecht, The Netherlands*

Received February 26, 2006; Revised Manuscript Received March 22, 2006

## ABSTRACT

We have studied the gate and temperature dependence of molecular junctions containing sulfur end-functionalized tercyclohexylidenes. At low temperatures we find temperature-independent transport; at temperatures above 150 K the current increases exponentially with increasing temperature. Over the entire temperature range (10–300 K), and for different gate voltages, a simple toy model of transport through a single level describes the experimental results. In the model, the temperature dependence arises from the Fermi distribution in the leads and in a three-parameter fit we extract the level position and the tunnel rates at the left and right contact. We find that these parameters increase as the bias voltage increases.

Understanding the conduction characteristics through single molecules is of crucial importance for further development of molecular electronics.<sup>1–3</sup> Temperature-dependent transport measurements<sup>4–7</sup> form a useful tool to distinguish between different mechanisms. For example, experiments on ensembles of alkanethiols<sup>4</sup> have shown temperature-independent electron transport indicative of a tunneling mechanism (superexchange). Selzer et al.<sup>5</sup> report on a crossover from temperature-independent transport at low temperature to an exponential dependence at temperatures above 100 K. They attribute this crossover to a change of conduction mechanism from tunneling at low temperatures to incoherent hopping transport at high temperatures induced by a coupling to vibrational states. Finally, scanning tunneling microscope measurements on single alkanedithiol molecules<sup>7</sup> show an exponential resistance dependence on temperature, which is attributed to a change in conformer distribution as the temperature is varied.

Here we report on the temperature dependence of three-terminal molecular junctions based on sulfur end-functionalized tercyclohexylidenes.<sup>8</sup> The rigid molecules possess

$\sigma$ - $\pi$ - $\sigma$  conjugation and consist of three cyclohexane-type rings<sup>9</sup> connected by double bonds (see Figure 1a). For low bias voltages, we observe temperature-independent transport at low temperatures and above a crossover temperature of about 150 K the current increases exponentially with the inverse temperature. A toy model based on transport through one molecular level provides a good fit to the data at all bias and gate voltages. We find that the tunnel couplings (broadening) increase as the bias is increased and that there is a weak shift of the level position as the bias increases. The level position deduced from the temperature-dependent fits agrees well with the level position determined from stability diagrams, in which  $dI/dV$  is plotted as a function of bias and gate voltage.

Electrodes with nanometer separation are fabricated by electromigration.<sup>10</sup> In short, we create a thin 10-nm-thick gold wire (width 100 nm, length 500 nm) on top of an Al/Al<sub>2</sub>O<sub>3</sub> gate electrode using e-beam lithography. The thin gold bridge is contacted by 100-nm-thick gold leads. To create a gap, a technique similar to that of Strachan et al. is employed.<sup>11</sup> At  $\sim 10^{-5}$  mbar the bridges are electromigrated at room temperature by ramping a voltage over the bridge using an active feedback loop: the voltage is ramped until a decrease in the conductance is observed, upon which the

\* Corresponding author. E-mail: hsjvanderzant@tnw.tudelft.nl.

<sup>†</sup> Delft University of Technology.

<sup>‡</sup> Condensed Matter and Interfaces, Utrecht University.

<sup>§</sup> Organic Chemistry and Catalysis, Utrecht University.

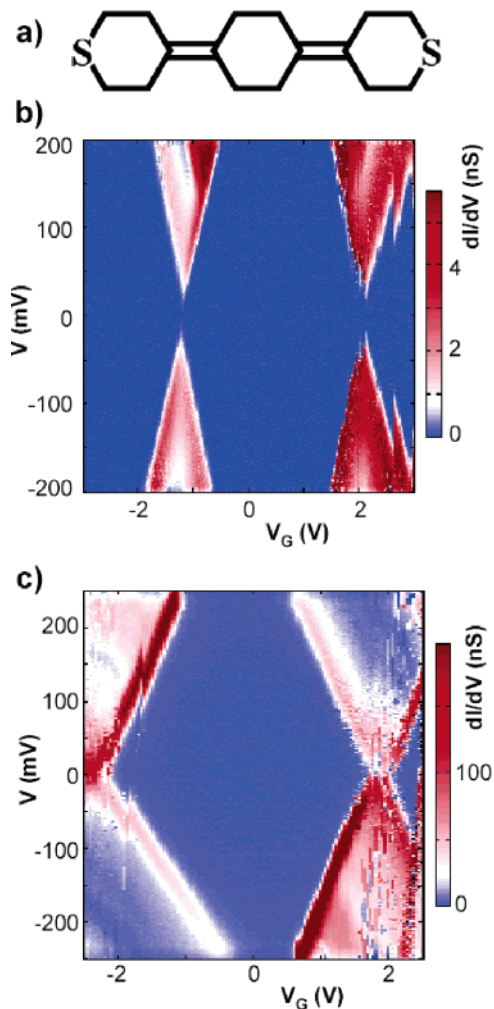


**Figure 1.** (a) Molecular structure of the sulfur end-functionalized tercyclohexylidene. (b and c) stability diagrams of sample A measured at 1.7 K and sample B measured at 8 K, respectively. Plotted is the numeric differential conductance ( $dI/dV$ ) in color scale as a function of source–drain and gate voltage. The gate coupling relating voltages on the horizontal gate axis to shifts in the level position is 0.15 (sample A) and 0.1 (sample B).  $G_{\max} = 0.04 \mu\text{S}$  (sample A) and  $G_{\max} = 0.9 \mu\text{S}$  (sample B).

applied voltage is returned to zero; the loop is repeated until a target resistance has been reached. The samples are then removed from vacuum and immersed in a 0.1 mM ethanol solution of the molecules for 12 h; thereafter the samples are dried and mounted in a probe station or a He-4 probe.

We have measured the current as a function of gate and bias voltage for hundreds of devices at low temperature. We found that in about 9% (42) of the 449 junctions the numerical derivative of the current to the bias voltage ( $dI/dV$ ) showed an appreciable gate dependence in the range from  $-3$  to  $+3$  V. Of these, 28% (12) of the junctions were too unstable to study the gate dependence in detail. In 31% (13) of the cases, multiple charge states (typically 5 or more) and addition energies smaller than 0.1 eV are observed.<sup>10</sup> These junctions most likely contain gold grains that dominate transport instead of the molecules. In the remaining 41% (17) 1 or 2 degeneracy points (crossing points of diamond-like structures, see Figure 1) are present with addition energies exceeding 0.2 eV; transport through these junctions

is attributed to transport through molecules, and the presence of closed diamonds (rhomboids) in the  $dI/dV$  diagrams indicate that it is dominated by a single molecule.<sup>12</sup>

The results of measurements on two stable junctions are shown in Figure 1b and c. The presence of closing diamonds indicates that in both cases a single island is present between the electrode pairs and that the addition energy<sup>12</sup> is about 0.5 eV for sample A and 0.4 eV for sample B. The two samples in Figure 1 have a relatively high gate coupling. In most other samples, the addition energy could not be determined: a lower gate coupling allows only a single degeneracy point to be observed or large and frequent switching occurred causing an offset along the gate axis. (In Figure 1b and c, a small switch is present in both figures.) In all cases, however, the data are consistent with an addition energy of 0.4–0.5 eV. Note that this addition energy cannot be compared directly with the measured HOMO–LUMO gaps of free molecules not attached to metal pads. The gold electrodes can lower the addition energies dramatically as indicated by the measurements on OPV-5 by Kubatkin et al.<sup>13</sup>

We have measured the current as a function of temperature for several gate and bias voltages. The most complete data set has been obtained for sample B, which we will discuss in the remainder of this paper. The data of sample A support the conclusions presented here. Figure 2 shows the current as a function of inverse temperature for four different bias voltages at two gate voltages on a semilog scale. The highest temperature is 240 K; when raised to this temperature we found the same transport characteristics at low temperatures after cooling again.

At low bias the curves in Figure 2 show thermally activated transport at high temperature and temperature-independent transport at low temperature. The crossover temperature is about 150 K in Figure 2a and decreases slightly as the bias is increased. The slope of the exponential increase above this crossover temperature yields an activation energy ( $E_a$ ) of 120 meV at low bias and this value decreases with increasing bias. At a bias of 200 mV, the current is almost temperature-independent for the curve taken at  $V_G = -1.0$  V. The same bias dependence of the slope and the crossover temperature are seen at other gate voltages.

To describe the temperature-dependent transport, we have considered a toy model<sup>14</sup> that includes a single transport level positioned at a gate-dependent energy of  $\epsilon_0$ , measured with respect to the chemical potential in the leads at  $V = 0$ , with a broadening  $\Gamma = \Gamma_L + \Gamma_R$ . Here,  $\Gamma_L/\hbar$  is the tunnel rate to the left electrode and  $\Gamma_R/\hbar$  to the right electrode. In this model the temperature dependence comes from the Fermi distribution,  $f(E)$ , in the leads; coupling to vibrational modes is neglected. The density of states is given by<sup>14</sup>

$$D(E) = \frac{1}{2\pi} \frac{\Gamma}{(E - \epsilon_0)^2 + (\Gamma/2)^2} \quad (1)$$

The current depends on the density of states within the bias

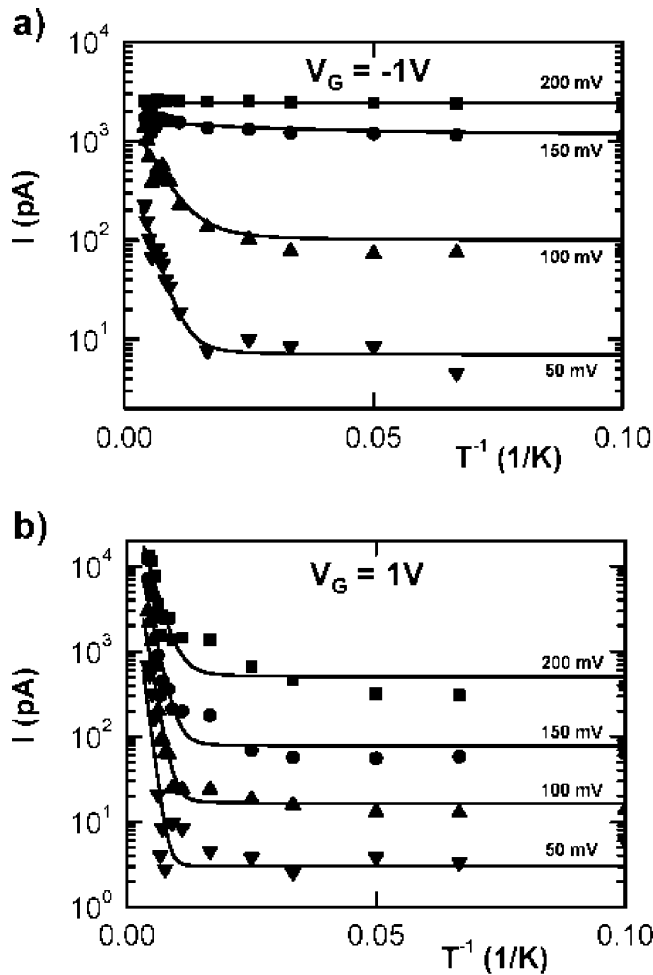


**Figure 2.** Current as a function of inverse temperature for four different source–drain voltages as denoted in the figures plotted for gate voltages of (a)  $-1.0$  V and (b)  $1.0$  V. Data are taken from sample B. Drawn lines represent the best fits of the data to the toy model with fit parameters  $\Gamma_L$ ,  $\Gamma_R$ , and  $\epsilon_0$ .

window, defined as the difference between the electrochemical potentials in the left and the right lead:

$$I = \frac{e}{\hbar} \int_{-\infty}^{\infty} D(E) \frac{\Gamma_L \Gamma_R}{\Gamma_L + \Gamma_R} [f(E - eV/2) - f(E + eV/2)] dE \quad (2)$$

Figure 3 shows the results of the calculated current versus inverse temperature at different bias voltages normalized to  $\epsilon_0$ . The results do not depend on the sign of  $\epsilon_0$ , and by definition  $\epsilon_0$  is taken to be positive. The overall shape of these curves can be explained as follows. At low bias ( $V \ll 2\epsilon_0/e$ ) and low temperatures, the current is due to tunneling with a rate determined by the broadenings  $\Gamma_L$  and  $\Gamma_R$  and the difference between  $\epsilon_0$  and the chemical potentials of the two leads. As long as the thermal energy,  $k_B T$ , is much lower than  $\epsilon_0$  and  $\Gamma$ , the current is temperature-independent. As the temperature increases, the step function of the Fermi distribution broadens. The current remains temperature-independent, until the high-energy (exponential) tail of the Fermi distribution of the highest electrochemical potential starts to overlap with the broadened level and the current

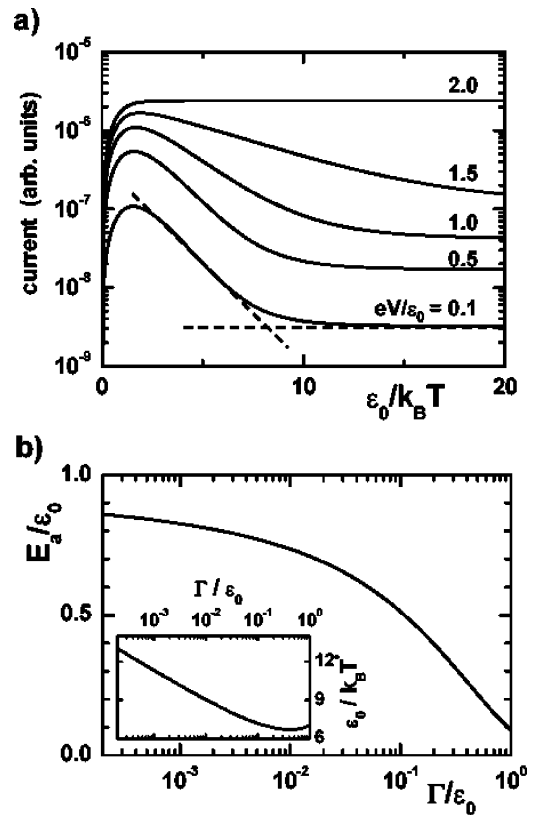


**Figure 3.** (a) Calculated current as a function of inverse temperature for five different values of the bias voltage  $eV/\epsilon_0$  for a broadening  $\Gamma/\epsilon_0 = 0.02$ . (b) The low-bias activation energy as a function of the broadening, all expressed in terms of  $\epsilon_0$ . Inset: the inverse crossover temperature as a function of the broadening.

increases exponentially with temperature (see Figure 3). This increase continues until the Fermi distribution of the other electrode overlaps with the broadened level. At this point, the current starts to decrease. However, when the level is resonant with the chemical potential in the leads ( $V = 2\epsilon_0/e$ ), the current is independent of temperature if  $T < 2\epsilon_0/k_B$ . Above this temperature, thermal smearing causes the current to decrease.

It may be expected that the crossover temperature,  $T^*$ , defined as the point where the zero temperature current crosses the tangent line with the highest slope in the thermally activated region, depends on the broadening of the level. We have calculated the crossover temperature numerically, and the result is shown in the inset of Figure 3b. We find that  $k_B T^*$  only weakly depends on  $\Gamma$  and that the exponential increase with temperature sets in at a temperature corresponding to an energy scale about 1 order of magnitude smaller than  $\epsilon_0$ . We have also calculated the slope of the exponential current increase at low bias, that is, the activation energy,  $E_a$ . For vanishing  $\Gamma$  the activation energy equals  $\epsilon_0$ , but as the ratio  $\Gamma/\epsilon_0$  approaches one the activation energy can be substantially smaller than  $\epsilon_0$ , as is illustrated in Figure 3b.

We have fitted our data to this model. The lines drawn in Figure 2 represent the best fits, which describe the data well. We have chosen two gate voltages far away from the two degeneracy points where variations in the current are large

**Table 1.** Fit Parameters for the Temperature-Dependent Current Plotted in Figure 2<sup>a</sup>

V (mV)	$V_G = -1.0$ V			$V_G = 1.0$ V		
	$\epsilon_0$ (meV)	$\Gamma_L$ (meV)	$\Gamma_R$ (meV)	$\epsilon_0$ (meV)	$\Gamma_L$ (meV)	$\Gamma_R$ (meV)
50	-63	0.003	2.3	119	0.10	0.10
100	-74	0.008	4.1	121	0.16	0.16
150	-77	0.007	5.1	133	0.28	0.29
200	-100	0.010	<170 <sup>b</sup>	146	0.30	1.26

<sup>a</sup> Equation 2 is symmetric in  $\Gamma_L$  and  $\Gamma_R$ , and we adopt the convention that  $\Gamma_L < \Gamma_R$ . The sign of  $\epsilon_0$  cannot be inferred from the fit; the slope of the diamond edges in Figure 1c has been used to determine it. <sup>b</sup> The current is almost temperature-independent in this particular case, implying that the energy level is located at the chemical potential of one of the contacts. In this case the fit procedure is not very sensitive to the value of  $\Gamma_R$  because a large range of values produces a good fit to the data; only an upper bound can be given.

and the fit procedure yields accurate values for the fit parameters  $\Gamma_L$ ,  $\Gamma_R$ , and  $\epsilon_0$ . The plots in Figure 2 probe two different levels, and the fit parameters are collected in Table 1. The total broadening,  $\Gamma$ , ranges from 0.1 to 5 meV and, interestingly, the values and the asymmetry between  $\Gamma_L$  and  $\Gamma_R$  differ for the two gate voltages. Another observation is that the tunnel rates,  $\Gamma_{L,R}/\hbar$ , increase with increasing bias voltage. In addition, the  $\Gamma/\epsilon_0$  ratio ranges from  $10^{-3}$  to  $10^{-2}$  and as Figure 3b indicates the measured activation energy,  $E_a$ , should be close to  $\epsilon_0$ . The measured  $E_a$  value of 120 meV is indeed in the same range as the values listed in Table 1. The level position can also be compared to values<sup>15</sup> independently determined from the stability diagrams in Figure 1. For all measurements, we find that they agree, to within a factor of 2, with each other, which is striking considering the simplicity of the model. Finally, the numbers in Table 1 also suggest that the level position is slightly raised with increasing bias. Shifting of the level position with bias has been predicted by quantum chemistry calculations for nonequilibrium transport through single molecules.<sup>16,17</sup>

Information on the value of  $\Gamma$  can also be obtained from the differential conductance peaks plotted as a function of bias voltage. If  $\Gamma > k_B T$  (this is the case for  $V_G = -1.0$  V; see Table 1) then a Lorentzian  $dI/dV$  peak shape is expected, and if  $\Gamma \approx k_B T$  ( $V_G = 1.0$  V) then the peak shape is the convolution of thermal and the lifetime ( $\Gamma$ ) broadening. As Figure 4 illustrates, a Lorentzian peak is indeed found in the former case with a broadening of 8 meV, close to the high-bias value of 5 meV. At  $V_G = 1.0$  V the peak shape is strongly asymmetric, prohibiting an accurate determination of  $\Gamma$ . The asymmetry can be attributed to phonon emission with  $\Gamma/h$  larger than the vibrational frequency in combination with an asymmetric<sup>18</sup>  $\Gamma_L$  and  $\Gamma_R$ . We have performed quantum chemistry calculations using Amsterdam Density Functional<sup>19</sup> (ADF) on a teracyclohexylidene molecule connected to gold atoms at either end that indicate vibrational modes at 6, 11, and 13 meV. With a broadening of several millielectronvolts, features related to these vibrational modes cannot be resolved but may produce the shoulder present in the data at the right-hand side of the peak. Interestingly, Figure 2b shows an enhancement of the current for  $T \geq 70$  K. This may have to do with the onset of phonon absorption

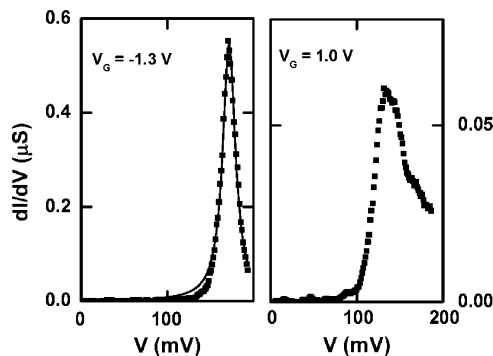


**Figure 4.** Differential conductance ( $T = 8$  K) of sample B as a function of positive source–drain voltage at a gate voltage of  $-1.3$  V (left) and  $1.0$  V (right). For the negative gate voltage the peak shape can be well fitted to a Lorentzian with  $\Gamma = 8$  meV (thin drawn line). A moving average filter has been applied to the data to calculate the numerical derivative. The averaging did not change the value of  $\Gamma$  significantly.

enabled by a temperature-induced population of the 6 meV and other low-lying vibrational modes.

Several explanations for voltage-dependent broadening are possible.<sup>20</sup> Conformational changes due to a larger polarization at applied fields may give rise to a better electrode–molecule coupling (and therefore broadening) at high bias. Another explanation involves the energy dependence of the density of states of the leads,<sup>21</sup> giving rise to a nonsymmetric dependence of the broadenings with bias. Estimates using a free electron model show that this may account for an increase in  $\Gamma$  of about 10% for typical parameters. We have also considered the effect of an energy dependence in the coupling between the leads and the molecule due to a change in the barrier shape as the bias is increased, using a simple tunneling model.<sup>22</sup> For a typical barrier height of a few hundred millielectronvolts, the increase in  $\Gamma$  is less than one percent, much smaller than the observed increase.

In conclusion, we have shown that the temperature dependence of the current through molecular junctions can be explained well with a toy model that involves a single transport level. Comparison of our data with this model yields important information about the level position and the broadening. We find that both parameters increase as the bias increases. To compare this voltage dependence with theory, a full self-consistent quantum chemical calculation of the coupled molecule/metal system is needed.

**Acknowledgment.** We thank Maarten Wegewijs for discussions and Jos Seldenthuis for performing the ADF calculations. Financial support was obtained from the Dutch Organization for Fundamental Research on Matter (FOM).

## References

- (1) Joachim, C.; Gimzewski, J. K.; Aviram, A. *Nature* **2000**, *408*, 541–548.
- (2) Nitzan, A.; Ratner, M. A. *Science* **2003**, *300*, 1384–1389.
- (3) Heath, J. R.; Ratner, M. A. *Phys. Today* **2003**, *May*, 43–49.
- (4) Wang, W.; Lee, T.; Reed, M. A. *Phys. Rev. B* **2003**, *68*, 035416.
- (5) Selzer, Y.; Cabassi, M. A.; Mayer, T. S.; Allara, D. L. *J. Am. Chem. Soc.* **2004**, *126*, 4052.



- (6) Stewart, D. R.; Ohlberg, D. A. A.; Beck, P. A.; Lau, C. N.; Stanlet Williams, R. *Appl. Phys. A* **2005**, *80*, 1379.
- (7) Haiss, W.; van Zalinge, H.; Bethell, D.; Ulstrup, J.; Schiffrin, D. J.; Nicols, R. J. *Faraday Discuss.* **2006**, *131*, 253.
- (8) We have also studied junctions with this type of molecule fabricated with a completely different method based on electrochemical etching: Kervennic, Y.-V.; Thijssen, J. M.; Vanmaekelbergh, D.; Dabirian, R.; van Walree, C. A.; Jenneskens L. W.; van der Zant, H. S. J. *Angew. Chem. Int. Ed. and Angew. Chem.*, in press (DOI: 10.1002/anie.200503591).
- (9) Marsman, A. W.; Havenith, R. W. A.; Bethke, S.; Jenneskens, L. W.; Gleiter, R.; van Lenthe, J. H.; Lutz, M.; Spek, A. L. *J. Org. Chem.* **2000**, *65*, 4584–4592.
- (10) van der Zant, H. S. J.; Kervennic, Y.-V.; Poot, M.; O'Neill, K.; de Groot, Z.; Heeersche, H. B.; Stuhr-Hansen, N.; Bjørnholm, T.; Vanmaekelbergh, D.; van Walree, C. A.; Jenneskens, L. W. *Faraday Discuss.* **2006**, *131*, 347.
- (11) Strachan, D. R.; Smith, D. E.; Johnston, D. E.; Park, T.-H.; Therien, M. J.; Bonnell, D. A.; Johnson, A. T. *Appl. Phys. Lett.* **2005**, *86*, 043109.
- (12) Natelson, D. Single-Molecule Transistors, chapter to be published in the *Handbook of Organic Electronics and Photonics*; Nalwa, H. S., Ed.; American Scientific Publishers, 2006.
- (13) Kubatkin, S.; Danilov, A.; Hjort, M.; Cornil, J.; Bredas, J. L.; Stuhr-Hansen, N.; Hedegård, P.; Bjørnholm, T. *Nature* **2003**, *425*, 698–701.
- (14) Datta, S. *Nanotechnology* **2004**, *15*, S433.
- (15) In conventional Coulomb blockade theory, the vertical distance at a particular gate voltage between the diamond edges equals  $4e_0/e$ .
- (16) Paulsson, M.; Stafström, S. *Phys. Rev. B* **2001**, *64*, 035416.
- (17) Xue, Y.; Ratner, M. A. *Phys. Rev. B* **2003**, *68*, 115406.
- (18) Braig, S.; Flensberg, K. *Phys. Rev. B* **2003**, *68*, 205324.
- (19) te Velde, G.; Bickelhaupt, F. M.; Baerends, E. J.; Guerra, C. F.; van Gisbergen, S. J. A.; Snijders, J. G.; Ziegler, T. *J. Comput. Chem.* **2001**, *22*, 931–967.
- (20) We have considered the role of Joule heating in the model; it produces a larger smearing of the Fermi distribution. Because the local temperature is higher than the measured one, the data points in Figure 2 should be shifted to the left-hand side. Fitting the one-level toy-model to the shifted data yields  $\Gamma_R, \Gamma_L$  values such that  $\Gamma = \Gamma_R + \Gamma_L$  increases and the ratio  $\Gamma_R\Gamma_L/(\Gamma_R + \Gamma_L)$  decreases as the bias is increased. The parameters in Table 1 do not show this trend, so heating most likely does not play a substantial role. For a proper description of heating in the molecule/metal system, however, inelastic processes should also be incorporated, which is beyond the scope of the present paper.
- (21) Newns, D. M. *Phys. Rev.* **1969**, *178*, 1123.
- (22) Simmons, J. G. *J. Appl. Phys.* **1963**, *34*, 1793.

NL0604513